MONITORING OF PRECIPITATION HARDENING IN AN HSLA STEEL THROUGH EMAT MEASUREMENTS OF MAGNETOSTRICTION*

B. Igarashi, G. A. Alers, and P. T. Purtscher
National Institute of Standards and Technology
Materials Reliability Division
Boulder, Colorado 80303

INTRODUCTION

This work demonstrates a novel application of ultrasound: measurement of magnetostriction, the change of length of a ferromagnetic material that accompanies a change in magnetization. The technique involves measuring ultrasonic waves generated by an electromagnetic acoustic transducer (EMAT), and it offers an alternative method of measuring magnetostriction in cases where it would not be feasible to use strain gages (for example, on fragile, thin films).

In this study, EMAT measurements of magnetostriction provide an NDE tool for probing the microstructure of steel. In particular, measurements are used to detect the formation of strengthening precipitates in an HSLA steel. The precipitates are Cu-rich precipitates (CRPS) that are too fine to be observed under an optical microscope. Results

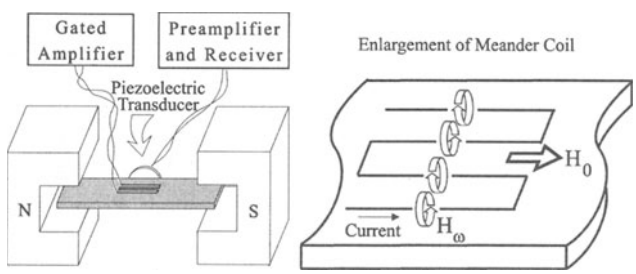

Figure 1. Setup for magnetostrictively generating SH_0 ultrasonic waves with an EMAT. The meander coil carries ac current, and H_0 is applied by an external electromagnet.

* Contribution of an agency of the U.S. Government, not subject to copyright.

Review of Progress in Quantitative Nondestructive Evaluation, Vol. 18
Edited by Thompson and Chimenti, Kluwer Academic/Plenum Publishers, 1999

of this investigation might prove to be relevant to inspection of reactor pressure vessel steel, which is embrittled by the formation of CRPs [1].

EMAT MEASUREMENT OF MAGNETOSTRICTION

Estimates of magnetostriction are obtained by measuring the amplitude of EMAT-generated plate waves. Thompson [2–4] has shown that shear horizontal (SH) plate waves can be generated magnetostrictively with the arrangement shown in Figure 1. A static tangential magnetic field H_0 applies tension or compression to the sample due to magnetostriction. The ac current in the meander coil creates oscillating fields H_ω that add perpendicularly to the static field and, in effect, locally rotate the axis of tension (or compression). These perturbations create shear strains that excite shear waves that propagate in the plane of the sample and also are polarized parallel to the surface of the sample.

In the experiments described below, we wish to excite the simplest mode of SH plate waves, the so-called SH_0 mode, where wave displacements are uniform through the thickness of the sample. In order to excite this mode, ac frequency f is set to $v_s/(2D)$, where v_s is the shear wave velocity (approximately 3.2 mm/μsec in steel) and D is the spacing between the long current elements of the meander coil. Since D is typically on the order of mm, f falls in the range, 100 kHz –1 MHz.

At these frequencies, ac field H_ω penetrates only 10—100 μm below the surface of the sample, as dictated by the electromagnetic skin depth, $\delta = \sqrt{1/(\mu_t \sigma \pi f)}$. In this expression, μ_t is the transverse incremental permeability and σ is the ac conductivity. (The transverse incremental permeability applies here, because the oscillating field H_ω is perpendicular to the static field H_0.) Hence, the magnetostrictive generation of SH0 waves occurs in a near-surface zone beneath the EMAT.

According to Thompson [2–4], the amplitude Ψ of SH waves generated magnetostrictively by the EMAT obeys the relationship,

$$\Psi \propto \delta h \left| \frac{\partial \varepsilon_{xy}}{\partial H_\omega} \right|, \tag{1}$$

where ε_{xy} is the magnetostrictive shear strain induced by H_0 and H_ω and h is the magnitude of H_ω at the sample surface. It has been shown recently [5] that near saturation fields H_0,

$$\frac{\partial \varepsilon_{xy}}{\partial H_\omega} \cong \frac{3}{2} \frac{\lambda}{H_\omega} \frac{\left(\frac{B_0}{\mu_t H_\omega} - \frac{\mu_t H_\omega}{B_0} \right)}{\left(\frac{B_0}{\mu_t H_\omega} + \frac{\mu_t H_\omega}{B_0} \right)^2}, \tag{2}$$

where B_0 is the magnetic induction due to H_0 and λ is the magnetostriction coefficient (the longitudinal strain due to H_0). The two expressions above show that magnetostriction coefficient λ is proportional to the wave amplitude:

$$|\lambda| \propto \Psi \sqrt{\mu_t} \frac{\left(\frac{B_0}{\mu_t H_\omega} + \frac{\mu_t H_\omega}{B_0} \right)^2}{\left| \frac{B_0}{\mu_t H_\omega} - \frac{\mu_t H_\omega}{B_0} \right|} . \qquad (3)$$

This expression is valid primarily at high H_0.

EXPERIMENTAL SET-UP

Descriptions of Samples

In this work, measurements are performed on two different types of steel: ultralow carbon (ULC) steel and A710 steel containing 1 mass % Cu. The ULC steel contains 0.003 mass % C, and its grain size is 12.9 μm. Our sample of this steel is a 26 x 13 x 0.08 cm plate that has been hot- and cold-rolled and annealed (with the rolling direction oriented parallel to the longest dimension of the sample). The top surface of the sample is wet-ground with 400 grit sandpaper and chemically polished with an aqueous solution of oxalic acid and hydrogen peroxide.

The A710 steel is a ferritic HSLA steel with nominal composition (in mass %): [C]=0.05, [Cu]=1.13, [Ni]=0.87, [Mn]=0.53, [Si]=0.30, [Cr]=0.75, [Mo]=0.21, [Nb]=0.32, [Al]=0.023. Three 122 x 21 x 9 mm bars with different states of Cu precipitation are available. These samples are described in detail elsewhere [6], but their characteristics may be summarized as follows:
(i) An underaged state is created by austenitizing the steel for one hour at 900 °C and then allowing it to air-cool. In this state, most of the Cu is in solid solution or it is trapped in tiny precipitates.
(ii) A peak-aged specimen is obtained by aging the steel at 525 °C for one hour. In this state, fine coherent Cu-rich precipitates (CRPs) with a diameter of about 5 nm form, and they introduce matrix strain that pins dislocations and increases the strength of the steel.
(iii) After aging the steel for one hour at 700 °C, an overaged state is obtained, in which the CRPs are more coarse and incoherent with the matrix. The matrix strain introduced by these coarse CRPs is much less than in the peak-aged state, and their strengthening effect is diminished.

Mechanical properties and x-ray diffraction measurements of the lattice strain of the A710 steel samples are given in Table I. The hardness values in the table correlate linearly with the lattice strains, and this suggests that the lattice strains reflect stresses from CRPs

Table I. Mechanical properties and lattice strains of A710 steel samples.

Specimen	Hardness (Rockwell A)	Proportional Limit (MPa)	Lattice Strain (10^{-4})
Underaged	55.6 ± 0.5	173 ± 10	6.9 ± 0.5
Peak-aged	58.5 ± 0.5	391 ± 10	7.4 ± 0.1
Overaged	53.2 ± 0.5	446 ± 10	5.3 ± 0.5

that pin dislocations and strengthen the steel. The proportional limits contained in the table are the maximum tensions that may be applied to standard tensile test specimens before the stress-strain curves deviate from linearity. It also should be noted that the grain size (approximately 10 μm) and the texture are nearly the same for all three samples. The heat treatments do not alter the microstructure of the steel (which is composed mainly of polygonal ferrite and some dispersed granular bainite).

Measurements are performed on a single surface of each sample that is wet-ground using a sequence of sandpapers decreasing in roughness from 60 to 800 grit. Subsequently, at least 30 to 40 μm of material is removed by chemically polishing the surface with an aqueous solution of oxalic acid and hydrogen peroxide. Between measurements, samples are stored under a roughing pump vacuum, and, after samples are exposed to air for a few hours during the course of conducting measurements, chemical polishing of samples is repeated.

Ultrasonic and Magnetic Measurements

The amplitude of SH_0 waves magnetostrictively generated by EMATs is measured in a pulse-echo experiment shown in Figure 1. A gated amplifier issues pulses consisting of a few cycles of sinusoids to a meander coil EMAT, and the amplitude of SH_0 waves excited by the EMAT is measured with a transverse piezoelectric transducer that is pressed flush against one edge of the sample and polarized parallel to the plane of the sample. The amplitude of waves is recorded as the static magnetic field H_0 provided by an electromagnet is decreased from saturation levels. During these measurements, the output of the gated amplifier is adjusted continuously to maintain a peak EMAT current of 5 A.

In the case of the ULC steel plate, a meander coil with grating spacing D of 3 mm (f = 551 kHz) is positioned in the middle of the plate, and the amplitude of SH_0 waves that are directly transmitted to the piezoelectric transducer is measured. Measurements are repeated with a meander coil that has spacing D of 9 mm (f = 170 kHz). In the case of the narrow A710 steel bars, a meander coil with grating spacing D of 2 mm (f = 791 kHz) is positioned

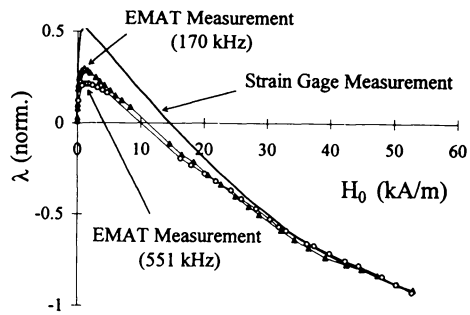

Figure 2. Estimates of the magnetostriction of the ULC steel yielded by the 170 kHz EMAT measurement (Δ), the 551 kHz EMAT measurement (o) , and the strain gage measurement (—).

a quarter wavelength away from one edge of the sample, so that the two pulses that are simultaneously emitted in opposite directions by the meander coil essentially combine to form a single pulse with approximately twice the duration. A clean first echo is observed, and its amplitude is recorded.

It should be noted that the amplitude of SH waves also could be measured by using an EMAT, thus, making the whole measurement noncontacting. However, it would be more difficult to extract the magnetostriction, since the wave amplitude would depend upon both the generation and reception efficiencies of the EMATs, which depend upon magnetostriction in different ways.

Values of the magnetic induction B_0 to be substituted into Equation (3) are derived from the B-H curve obtained by measuring the voltage induced across a solenoid wrapped around the sample. The transverse incremental permeability μ_t is measured through an eddy current technique, and the magnetostriction of the ULC steel plate is measured with strain gages. Details of these measurements are given in a previous work [7].

During all ultrasonic and magnetic measurements, samples are mounted between C-shaped pole pieces of the electromagnet (see Figure 1). Samples are positioned carefully in such a way as to minimize pulling on the ends of the sample due to magnetic attraction between the sample and the pole pieces.

ESTIMATES OF THE MAGNETOSTRICTION OF ULC STEEL

Estimates of the magnetostriction of the ULC steel plate obtained from EMAT and strain gage measurements are shown in Figure 2. The EMAT estimates result from substituting into Equation (3) measurements of the magnetic induction B_0, transverse incremental permeability μ_t, and the wave amplitude Ψ for the two different meander coils. In Equation (3), H_ω is taken to be the field at the skin depth, h / e. For the meander coil that is excited at 551 kHz, h is calculated from an available formula [4] to be 0.87 kA/m per ampere of current in the coil. The same formula gives h = 0.19 kA/m per ampere of current in the meander coil that is excited at 170 kHz. Positive and negative signs of the EMAT estimates of magnetostriction are assigned to data points on opposite sides of the fields where SH_0 waves undergo a 180° phase change. All curves in Figure 2 are normalized with respect to values measured at the highest magnetic field.

EMAT estimates of the magnetostriction agree well with the strain gage measurement at near-saturation magnetic fields, but at low fields, the EMAT measurements underestimate the positive magnetostriction. This discrepancy might be due to the fact that magnetic domain wall motion is suppressed when magnetic fields oscillate at 551 or 791 kHz; thus, one would not expect to observe the same positive contribution to magnetostriction from domain wall motion at low H_0 as during a static strain gage measurement. The EMAT estimates might agree better with the strain gage measurement at low fields, if the EMAT measurements were conducted at lower frequencies, where domain wall motion is not suppressed as much. There is already some evidence in Figure 2 that suggests this might be true: the 170 kHz measurement agrees slightly better with the strain gage measurement than the 551 kHz measurement does. It should be pointed out that, even though the low-field peak in the magnetostriction is underestimated by the EMAT measurements, the field at which it occurs still is predicted correctly.

One should keep in mind that the EMAT measurements yield estimates of the magnetostriction of just the near-surface zone of the sample. The wave amplitude reflects the magnetostriction of the region where waves are excited; namely, within the skin depth of the sample.

DETECTION OF STRENGTHENING PRECIPITATES IN A710 STEEL

Figure 3 shows results of measurements conducted on the three different samples of A710 steel. Figure 3(c) shows estimates of magnetostriction that are derived by substituting data from Figures 3(a), (b), and (d) into Equation (3) One observes that, while all of the magnetic properties are sensitive to the state of Cu precipitation, magnetostriction shows the largest sensitivity. While differences among the transverse incremental permeabilities and B-H curves of the three samples occur primarily at low H_0, differences among the magnetostriction curves extend to high fields.

Certain features of the magnetostriction and transverse incremental permeability change monotonically with the lattice strain, hardness, and proportional limit. For example, Figure 4 shows that the field at which the low-field peak in the magnetostriction occurs correlates linearly with the proportional limit. Figure 5 shows that the maximum

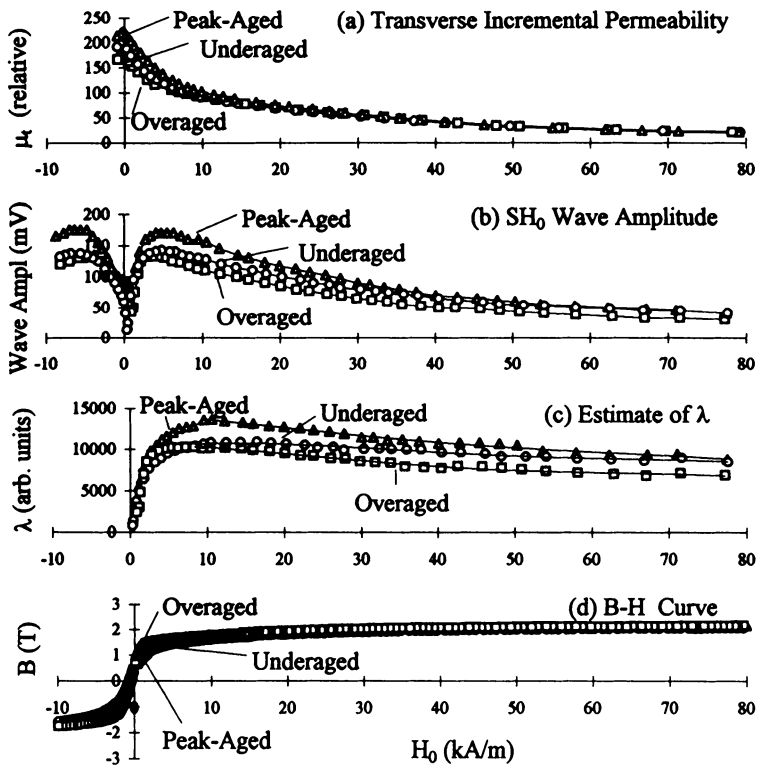

Figure 3. (a) Transverse incremental permeabilities, (b) SH_0 wave amplitudes, (c) estimates of λ from Equation (3), and (d) B-H curves obtained in the underaged (o), peak-aged (Δ), and overaged ($\square$) A710 steel samples.

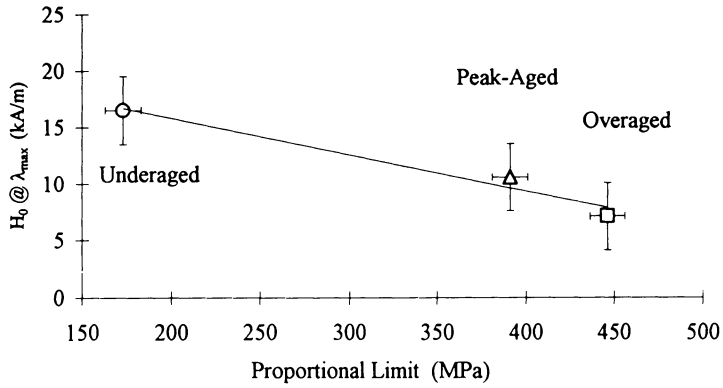

Figure 4. Magnetic fields H_0 of low-field peaks in Figure 3(c) vs. the proportional limits of the underaged (o), peak-aged (Δ), and overaged (□) A710 steel samples.

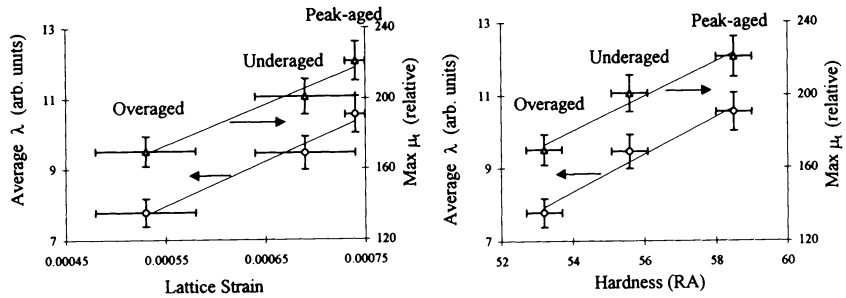

Figure 5. Estimated λ averaged over high H_0 (o) and maximum transverse incremental permeability (Δ) vs. lattice strain and hardness.

transverse incremental permeability and the average magnetostriction increase monotonically with the lattice strain and hardness. (The average magnetostriction is calculated over the near-saturation regime (above 25 kA/m, in this case), which is the range of the most valid estimates of λ in Figure 3(c).) The highest values of the transverse incremental permeability and the magnetostriction occur in the sample with the highest lattice strain and hardness.

It was suggested earlier that lattice strains reflect the very stresses from CRPs that pin dislocations and strengthen the steel. These stresses from CRPs also may affect domain wall motion and rotation of magnetic domains. This would explain why magnetic produce larger changes in the transverse incremental permeability and magnetostriction. However, it currently remains unclear why stresses from CRPs increase the average magnetostriction and incremental permeability.

This gap in our understanding does not prevent us from applying these results, though. The upshot is that EMAT measurements of magnetostriction can be used to monitor the

evolution of CRPs in this steel alloy. As a side benefit, one might use these correlation curves to predict the hardness and proportional limit of this steel alloy.

CONCLUSIONS

EMAT measurements may be used to determine key features of the magnetostriction of steel. Estimates of the relative magnetostriction are most accurate at near-saturation magnetic fields, and, although the low-field peak tends to be underestimated, the field at which it occurs is predicted correctly.

EMAT measurements of magnetostriction can be used to monitor the evolution of CRPs in A710 steel. The high-field average magnetostriction changes linearly with the lattice strain and hardness introduced by CRPs. The peak-aged state occurs when the high-field average magnetostriction is maximized. Results of this investigation suggest that EMATs might be useful for inspecting nuclear reactor pressure vessels to locate zones of irradiation-enhanced embrittlement caused by the formation of CRPs. This technique has the advantage of measuring the magnetostriction in the near-surface zone, which is where one would expect to find the majority of irradiation damage.

ACKNOWLEDGMENTS

We thank R. B. Thompson, J. H. Rose, C.-C. Tai, and J. C. Moulder of Iowa State University for their technical advice. We also thank D. Balzar, F. R. Fickett, J. D. McColskey, C. McCowan, W. L. Johnson, S. R. Schaps, and C. M. Fortunko of NIST-Boulder for their technical help. This work was funded by the Nuclear Regulatory Commission Program RES-97-005 (USA).

REFERENCES

1. G. R. Odette and G. E. Lucas, J. Nondestructive Eval. 15, 137 (1996).
2. R. B. Thompson, in: *1978 Ultrasonics Symposium Proceedings*, Cat. No. 78CH1344-1SU, eds. J. deKlerk and B. R. McAvoy (IEEE, New York, 1978), p. 374.
3. R. B. Thompson, Appl. Phys. Lett. 34, 175 (1979).
4. R. B. Thompson, in: *Ultrasonic Measurement Methods*, Vol. 19 of Physical Acoustics, eds. R. N. Thurston and A. D. Pierce (Academic Press, Boston, 1990), p. 157.
5. B. Igarashi, G. A. Alers, and P. T. Purtscher, in: *1997 IEEE Ultrasonics Symposium Proceedings*, eds. S. C. Schneider, M. Levy, and B. R. McAvoy (IEEE, New York, 1997) p. 709.
6. H. I. McHenry and G. A. Alers, "Nondestructive Characterization of Reactor Pressure Vessel Steels: A Feasibility Study," NIST Technical Note 1500-4, 1998.
7. B. Igarashi, G. A. Alers, and P. T. Purtscher, in: *Review of Progress in QNDE*, Vol. 17, eds. D. O. Thompson and D. E. Chimenti (Plenum, New York, 1998), p. 1485.